Available online at www.sciencedirect.com

ScienceDirect

Procedia CIRP 94 (2020) 769–774

www.elsevier.com/locate/procedia

11th CIRP Conference on Photonic Technologies [LANE 2020] on September 7-10, 2020

Process control by real-time pulse shaping in laser beam welding of different material combinations

Marc Seibold[a,]*, Hannes Friedmann[a], Klaus Schricker[a], Jean Pierre Bergmann[a]

[a]*Technische Universität Ilmenau, Department of Mechanical Engineering, Production Technology Group, 98693 Ilmenau, Germany*

* Corresponding author. Tel.: +49-3677-693829; fax: +49-3677-691660. *E-mail address:* marc.seibold@tu-ilmenau.de

Abstract

Joining of metallic material combinations with limited solubility is a challenging task. Because of low solubility, such material combinations lead to the formation of intermetallic compounds (IMC) during common weld bath. IMC then lead to increased hardness and brittleness. Generally, these properties are undesirable and the aim is to reduce intermetallics to a minimum. In this contribution, a process control by real-time pulse shaping is realized, whereby the power is adjusted in each individual pulse. The material-specific emissions are continuously detected by photodiodes and used as control variable. By equipping the photodiodes with band-pass filters, the wavelength can be selected in a material-dependent manner. The control loop including data processing and pulse shaping as well as the connection to the power supply of the laser beam source is realized by a novel system in less than 10 µs. This enables laser welding of different metals with a nearly constant penetration depth at the boundary layer and, therefore, the limitation of IMC.

Keywords: real-time pulse shaping, laser beam welding, pulsed welding, material specific emission, intermetallic compounds, process controll, interface

1. Introduction

Aluminum is a material widely used in several applications, e.g. as conductor material in electrical system, power technology or housings. In order to adjust certain properties, aluminum is often used in combination with other metallic materials, leading in many cases to the formation of intermetallic compounds (IMC). Examples of hybrid joints are the specific adjustment of electrical properties, thermal conductivity, damping and chemical resistance. In the ideal case, these properties require a firm bonding between both joining partners, which is challenging, when IMC are formed. Such intermetallics have a high-level of electrical and thermal conductivities as well as high brittleness and hardness [1]. Therefore, the main challenge in joining such dissimilar material combinations is the minimization of such intermetallic compounds.

Especially, when joining aluminum with copper [2] and with steel [3, 4], the resulting limited solubility is the cause of formation of IMC. Depending on the mixing ratio, several different intermetallics are formed which lead to a brittle fracture within the joining area and high electrical resistance [1].

These challenges will be illustrated by using aluminum-copper joints as an example. The formation of such IMC should therefore be limited in joining processes to achieve ductile failure and well-suited electrical and thermal properties [5]. Therefore, different approaches are followed in the state of the art.

In order to prevent the formation of IMC, the mixing of the joining zone is sought to be strongly reduced. Laser beam joining has the advantages of high flexibility, minimal process forces, high energy density and fast process speed. But the production of a common melt pool between two joining

10.1016/j.procir.2020.09.137

partners is disadvantageous, for example, compared to solid state joining processes [6]. Nevertheless, there are approaches for laser beam welding to address the challenges mentioned: The presence of the keyhole in deep penetration welding supports mixing in the melt pool [7, 8]. This can be further assisted by local beam oscillation [9]. During the laser beam deep welding, the keyhole supports mixing in the melting pool [7, 8]. Incidentally, a lateral offset of the laser beam in butt joint configurations shows comparable advantages, too [10].

Welding in overlap configuration, therefore, requires a precise knowledge of the welding process, especially the moment, when the lower joining partner is reached, heated and molten through the laser.

The detection of this particular instant of time is feasible by evaluating the process emission in the visible spectrum (VIS) [11, 12]. During the welding process, material-specific emissions can be detected by spectrometry as shown in figure 1. The multiple peaks around 450 nm to 560 nm are significant as they stand for Al2O3 emission. The double peak at 394.4 nm and 396.15 nm is also known to be pure aluminum [12, 13]. Compared to the integral plot over 1 min as shown in figure 1, time-resolved observation is also possible.

A time-resolved observation of the process emission is achieved by using photodiodes. Due to their high sampling rates and by applying suitable band-pass filters, specific wavelengths of materials can be addressed [11, 12, 14]. This allows the time-dependent identification of the respective material to be welded into [15][16].

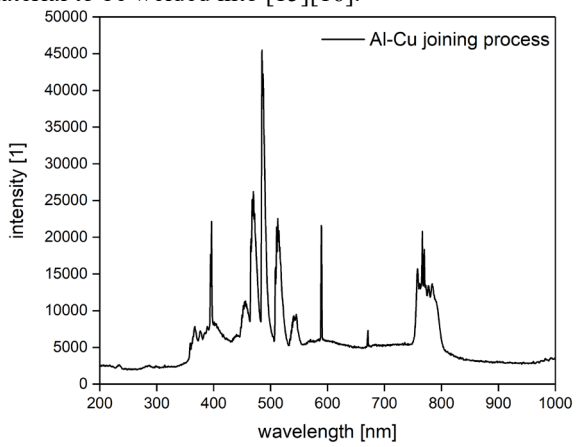

Fig. 1. VIS-spectrometry of aluminum-copper weld (signal average over 1 ms).

Pulsed laser beam welding offers the possibility of controlling the laser beam power input depending on these points in time for every pulse. However, previous investigations suffered from too long control time and time-lagged laser beam sources which can typically control the beam power at time intervals of 50 µs. The unstable process conditions during the welding of aluminum increase these requirements even further [3].

In this paper, the development of a process control for pulsed laser beam welding, which allows the minimal melting of the lower joining partner at the interface by addressing control times below 10 µs, is presented (figure 2). An analog-to-digital converter processes the emissions measured by means of photodiodes, suitable band-pass filters and, based on this, provides the pulse shape for the laser beam source. The process control should be used to generate a welding penetration depth close to the boundary surface and thus minimize the mixing. By implementing the control loop, it may be possible in future investigations to limit the formation of intermetallic phases due to the minimized mixing of both materials.

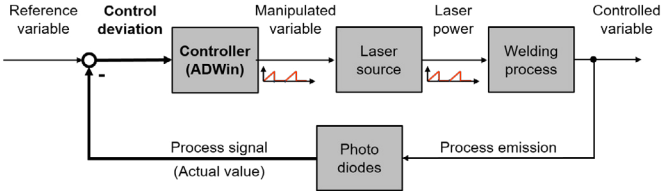

Fig. 2. Schematic illustration of the control loop being used.

2. Experiments

The laser beam source used is YLR-450/4500-QCW-MM-AC-Y14 from IPG Photonics with a maximum laser beam power of 4,500 W and maximum pulse energy of 45 J at a wavelength of 1,070 nm. This Q-switched laser has a power supply with a control frequency of 100 kHz which is much faster than conventional laser beam sources. Therefore, minimum control times of 10 µs can be addressed, whereas the laser power supply of conventional laser beam sources have a maximum control frequency of 20 kHz, resulting in a control time of 50 µs [18]. An optical fiber with a diameter of 200 µm was used. The collimation lens has a focal length of 85 mm and the focusing lens of 200 mm. This results in a focal diameter of approx. 470 µm.

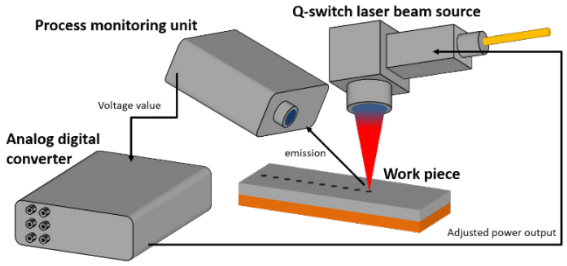

Fig. 3. Schematic illustration of the experimental setup.

All welds have been carried out in an overlap configuration as shown in figure 2. Three materials were used for the welds. EN AW 1050 (Al 99.5, see [19]) was used on the side of the aluminum and in all cases as the upper joining partner. Copper EN CW004A with residual oxygen was selected as the lower joining partner because this material combination was primarily used in battery production and for electrical contacts. Furthermore, steel 1.0330 (DC 01, see [20]) was used as an alternative lower joining partner to provide general validity of results.

A continuously rising ramp was chosen as a model like pulse shape in order to obtain the best results from the detection of emission in preliminary investigations [11]. This behavior can be explained by a slowly and continuously evolving laser process. The ramp starts at 0 W and increases up to 4,200 W. All pulses had the same maximum pulse duration of 5 ms. Equal power was applied to all welds, aluminum-copper and

aluminum-steel. This predefinition is assumed not to be critical because the laser beam power is controlled and switched down after reaching the interface within the lap joint.

For the detection of process emission, two photodiodes with different band-pass filters were used. BPW 21 type photodiodes were used due to their maximum photosensitivity at 550 nm [21]. This type is especially suitable for detecting the wavelength of 485 nm which is characteristic of several aluminum oxides.

A band-pass filter with 485 nm – 20 nm and a notch filter with 1,064 nm – 40 nm were used. The notch filter allows the entire emitted spectrum to be monitored which is within the sensitivity range of the photodiode while excluding the laser wavelength of 1,070 nm. This procedure allows the determination whether addressing individual, material-specific wavelengths is appropriate or whether the entire emission spectrum should be taken into account for process control.

In order to ensure that both diodes observe the same part of the process, they are mounted onto the beam splitters with different transmittance and reflectance coefficients (see figure 3). The first beam splitter shows reflectance of 30 % and transmittance of 70 %. The second beam splitter reflects and transmits the beam at 50 % each. Therefore, the photodiodes with band-pass filter have an illumination power between 30 % and 35 %. A pilot laser was used for the adjustment which emitted backwards through both beam splitters. The optical elements were so adjusted that the whole melting pool and metal vapor could be detected.

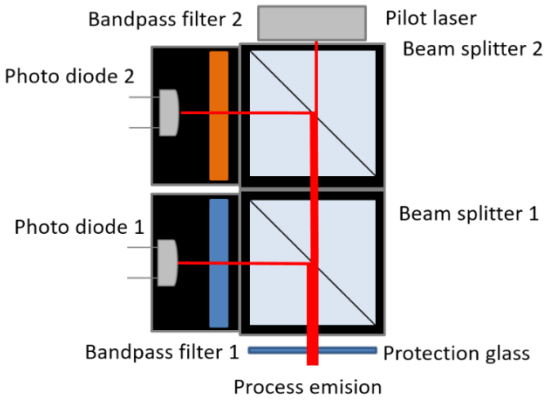

Fig. 4. Schematic illustration of the case with the optical components.

The controller is the analog-to-digital converter ADWin from Jäger Messtechnik. The processor T12 reaches a maximum cycle frequency of 1 GHz. The signal acquisition and data handling, the control system and the resulting pulse shape (power over time) for the laser beam source are processed by the ADWin system. It helps to achieve a minimum cycle time of 5 µs which is half the cycle time of 10 µs of the laser beam source and, therefore, fast enough to realize the process control.

The photodiodes output voltages are in the millivolt range. The controller operates within a voltage range of 0-10 V. In order to make the low voltage change usable as control variable, a transimpedance amplifier is used. The amplification factor of the circuit can be adjusted variably. For this purpose, the electrical resistance of the resistor can be changed. The electrical resistance is adapted to the emission signal.

The Q-switched laser beam source helps realize in-pulse power control. The chosen control strategy for the pulses is actually interruption control; thus, the power is set to 0 W when a critical control value is reached. So the energy of the pulse is variable and adjusted to each single pulse as result of the control.

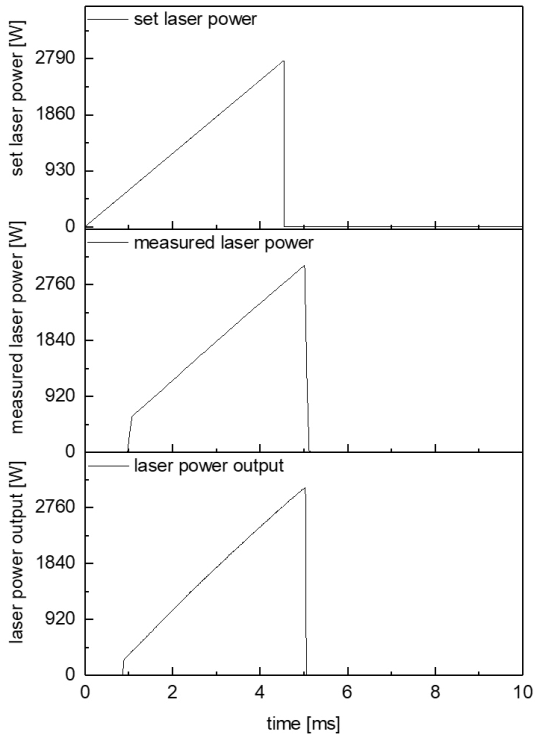

Fig. 5. Display of the results from the power measurement. 1. Figure: value of set laser power. 2. Figure: measured laser power. 3. Figure: analog laser power output value

The set value of laser beam power is given by the ADWin system and the resulting beam power is provided by the laser beam source via an analog output signal. In order to ensure that the power output signal corresponds to the real laser beam, the signal is compared to power measurements. These measurements are carried out by a Coherent PowerMax-Pro USB/RS which enables the time-dependent acquisition of the beam power. Due to the sampling rate of 20 kHz, the power increase is resolved with sufficient accuracy. Figure 4 depicts the comparison of a power ramp with the duration of 5 min and a maximum power of 3000 W. The power is not output from 0 s, but delayed by 0.87 min which corresponds to a beam power of 440 W. This effect is based on the threshold value of the laser beam source. From this point in time, a linear increase in power can be seen. The power curve, the maximum power and the time of pulse end follow the real value adequately. Therefore, the analog output of the laser beam source is considered sufficient for representing the laser beam power.

3. Results and discussion

3.1. Initial situation of uncontrolled process and assignment of different process stages to emission signals

The initial situation of a static, uncontrolled pulsed laser welding process is given in the following. Figure 5 shows a signal of an aluminum-to-copper spot weld. The recorded values of the set value of laser beam power, the laser beam power output, process emission at 485 nm and the notch filter are shown one below the other. It is easy to see that there is no specific emission at the signal of the notch filter. It is not possible to build a control system on this signal path. Therefore, only the emission at 485 nm will be shown in the further figures. In addition, the signal curve of the process emission at 485 nm is represented by a fitted curve, which symbolizes the generally valid signal and can be traced back to significant process events.

The set laser power from ADWin system defines the start time of the figure. The first red dotted line represents the point in time when the power reaches the threshold value of the laser beam source and the power is actually emitted. From this point in time on, the power output follows the set value.

The process emission at 485 nm is found to get delayed. This can be correlated to the point in time when the vaporization of the upper joining partner begins. The signal rises to a local maximum (1) (approx. 2.5 ms) and then drops again. Thus, the transition between heat conduction welding and deep penetration welding in the upper joining partner can be detected. The second more significant rise (2) results in a global maximum of the emission signal at approx. The maximum at 4,175 ms represents the progression in welding depth in the upper joining partner as the power continues to increase in parallel. On exceeding the maximum, the lower joining partner is reached. The conditions in the keyhole change or, respectively, the keyhole formation starts in the lower joining partner, which leads to a significant difference in the emission signal. Therefore, the subsequent drop represents the welding process in the lower joining partner. This behavior is comparable to the drop after the first local maximum at reduced power.

When the end of the pulse is reached, the emission also decreases rapidly. The signal does not suddenly drop to zero as the closing of the keyhole, the solidification and further cooling take a few tenths of a millisecond. The fitted curve also depicts the signal course sufficiently well. Also, a trigger value is set to 2.75 V after the peak has been exceeded as this is always below the previously occurring maximum. The voltage value is experimental to ensure that the maximal value of a given maximum is a global maximum.

The consideration of the total emission by using the notch-filter (1064 nm) of the process is not appropriate here as there is no allocation to all relevant process events.

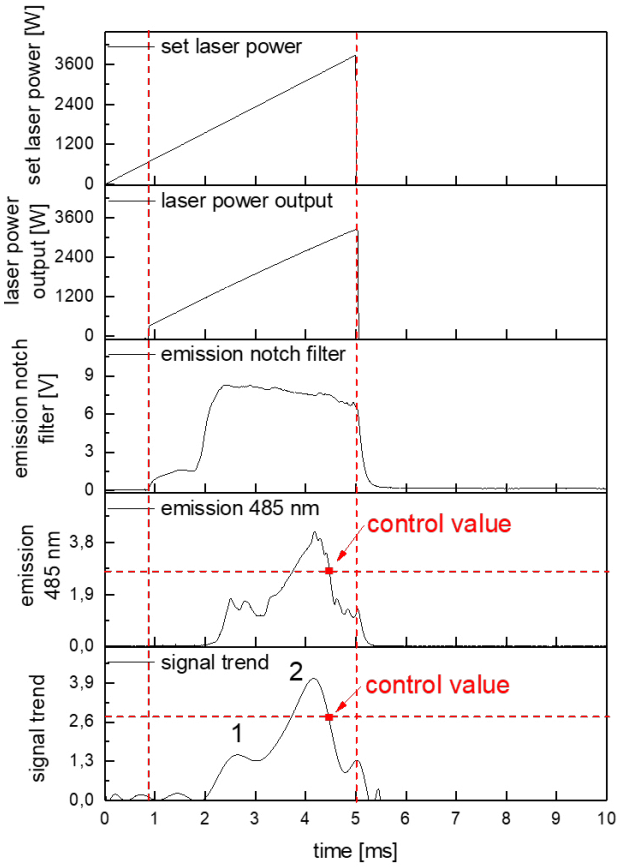

Fig. 6. Overview of all detected signals and the signal trend of the emission at 485 nm

Furthermore, the results are cross-checked by welding an aluminum-steel joint in an uncontrolled manner (see figure 6). It is noticeable that the process emission at 485 nm is comparable to the results gained by aluminum-copper welds. The emission curve is almost similar to the results provided in figure 5. The signal course is associated with the same events and also matches the fitted curve. This implies that process control can be implemented independent of the materials used.

Since laser beam power and process emission of 485 nm correspond so closely for different material combinations, power control is implemented based on a falling edge in the laser pulse.

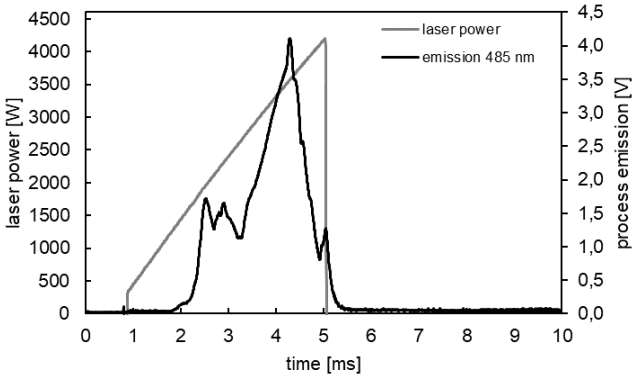

Fig. 7. (grey) laser power out from the laser beam source. (black) unregulated process emission

3.2. Process control

The implementation of the process control is shown exemplarily for welding of aluminum-copper and aluminum-steel joints. Based on the fitted emission curve, suitable trigger values for power control could be determined. Therefore, the controller lowers the laser beam power to the value of 0 W as the emission signal drops to the voltage value 2.75 V exceeding the global maximum emission peak. The voltage value for the regulation is adjusted to the amplification factor of the transimpedance amplifier. Therefore, the voltage value is only useful in this separate case.

Figure 7 shows the output laser beam power and the process emission at 485 nm of the controlled aluminum-copper weld. It can be seen by the laser power output that the termination criterion is reached after 4.38 ms when the power output is terminated.

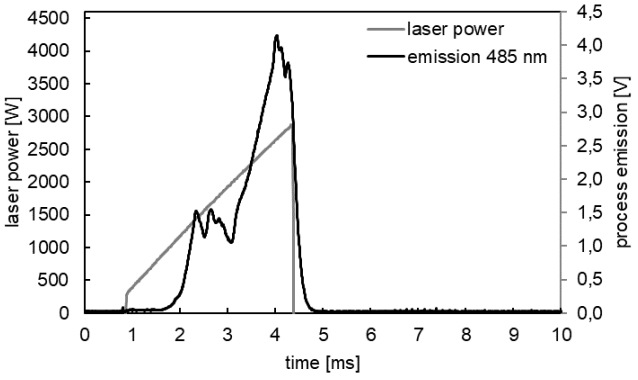

Fig. 8. Emission signal of a laser power based controlled weld with aluminum as upper and copper as lower sample

Figure 8 shows a controlled aluminum-steel weld. Again, the trigger voltage of the emission signal was set to 2.75 V as with the Al copper welding before due to the comparably identified process stages. The emission curve of the controlled process also resembles the curve of the aluminum-copper joints given in figure 7, as already seen in the uncontrolled process.

This confirms that control of the process is possible regardless of the material of the lower joining partner.

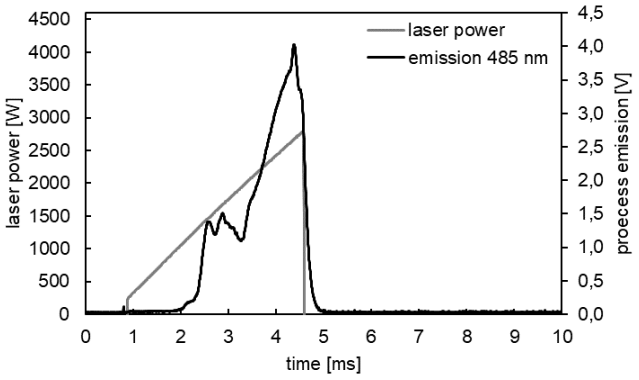

Fig. 9. Emissions signal of a controlled aluminium-steel weld

The diagrams shown demonstrate the possibility of implementing real-time pulse control on different material combinations. However, the signal curve provides no information about the weld itself. No statements can be made about the size of the joining zone or the mixing ratio of the materials at this time.

For further understanding, microsections were prepared out of the center of the spot welds for uncontrolled and controlled welding processes. In the case of uncontrolled process (see figure 9 a), the melted area in copper is smaller than that for aluminum. There is a darker area at the bottom of the weld which usually represents the formation of intermetallic compounds. Adjacent to it are yellow areas (see figure 9 d) that are typical for aluminum bronze [22].

The microsection of the controlled process is given in figure 9b. Primarily, it shows that only a minor proportion of copper was melted. This corresponds to the desired goal of a small weld in the lower joining partner. Incidentally, the small connected area between the sheets is disadvantageous. Due to the minimized weld penetration, potential cracks will still form in the interface between the sheets. These factors can lead to a reduced strength of the joining zone. A first starting point is the variation of the trigger values to improve the connection area. Further investigations are therefore required into this topic.

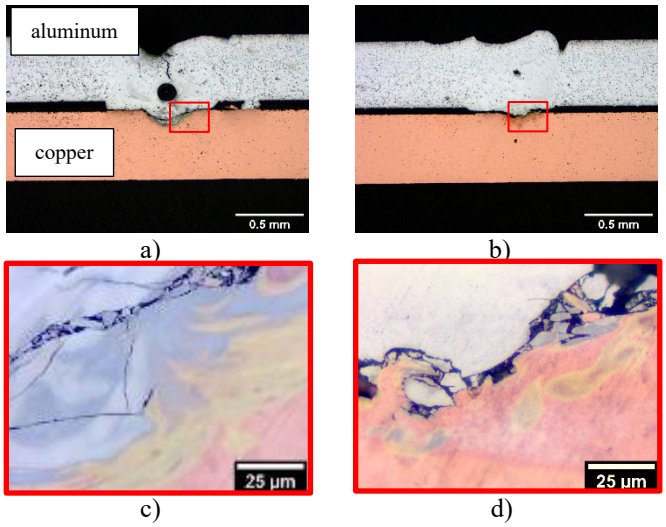

Fig. 10. aluminum copper welds (a) without power control; (b) with power control.

In comparison to the aluminum-copper weld, the welding depth for aluminum steel welding, by the same pulse shape, increases. This can be explained by the lower absorption of copper compared to steel [23, 24]. Figure 10 a) shows an uncontrolled aluminum-steel weld. In the given example, the spot weld is dominated by a pore in the entire area of the steel material. These pores appear regularly and thus significantly reduce the weld quality. In contrast, pore formation is not detected in the controlled weld (figure 10 b), d)). In addition, only a minor proportion of the lower joining partner is recognized. Again, the controlled weld also shows a smaller weld interface and a smaller supporting cross-section.

It can be stated that in-pulse power control can be applied in process technology and can be used in a material-independent manner. Future work must focus on the material issues related to a sufficient connection between both joining partners and characterization of the intermetallic compounds.

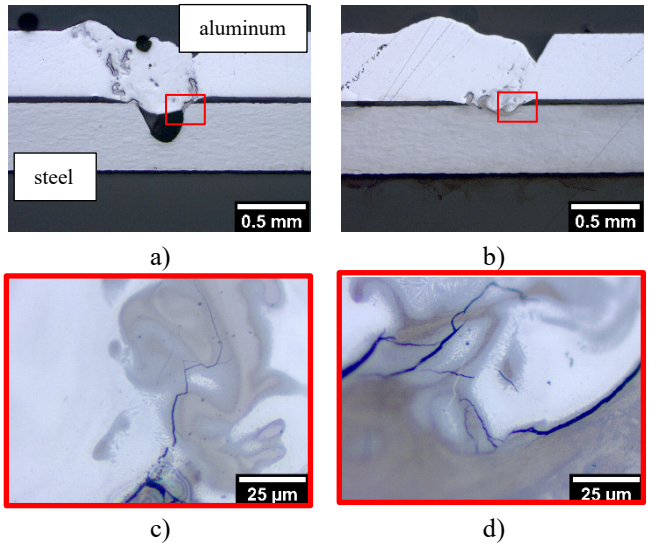

Fig. 11. aluminum steel welds (a) without power control; (b) with power control.

4. Conclusion

In summary, it has been shown that the steps of the welding process can be captured and recognized by using photodiodes in combination with band-pass filters. The signal waveform is independent of material compounds and is process oriented. By using signal amplification and a controller, a break-off control could be implemented. A comparison with the micrographs could show that the control leads to a lower weld penetration in the lower joining partner and, in the case of aluminum-steel mixed joints, to minimization of the pores. A disadvantage is that the resulting joining area has a small load capacity due to the small melted area.

Acknowledgements

We thank the Federal Ministry for Economic Affairs and Energy (BMWi) within the Zentrales Innovationsprogramm Mittelstand (ZIM) for funding the project. (FKZ 16KN053046)

References

[1] Braunovic, M.Aleksandrov, N. Intermetallic compounds at aluminum-to-copper and copper-to-tin electrical interfaces. 1992
[2] Bergmann, J. P.,Petzoldt, F.,Schürer, R.Schneider, S. Solid-state welding of aluminum to copper—case studies. Welding in the World. 2013 4. p. 541–550
[3] Kotadia, H. R.,Franciosa, P.Ceglarek, D. Challenges and Opportunities in Remote Laser Welding of Steel to Aluminium. MATEC Web of Conferences. 2019 10. p. 2012
[4] Ebhota, W. S.Jen, T.-C. Intermetallics Formation and Their Effect on Mechanical Properties of Al-Si-X Alloys. 2018
[5] Mathew, J.,Remy, G.,Williams, M. A.,Tang, F.Srirangam, P. Effect of Fe Intermetallics on Microstructure and Properties of Al-7Si Alloys. JOM. 2019 12. p. 4362–4369
[6] Köhler, T.,Raab, M.,Regensburg, A.Bergmann, J. P. Liquid interlayer formation during torsional ultrasonic welding of EN CW004A and EN AW1050. Welding in the World. 2019 5. p. 1187–1194
[7] Fetzer, F.,Jarwitz, M.,Stritt, P.,Weber, R.Graf, T. Fine-tuned Remote Laser Welding of Aluminum to Copper with Local Beam Oscillation. Physics Procedia. 2016. p. 455–462
[8] Hollatz, S.,Heinen, P.,Limpert, E.,Olowinsky, A.Gillner, A. Overlap joining of aluminium and copper using laser micro welding with spatial power modulation. Welding in the World. 2020 3. p. 513–522
[9] Jarwitz, M.,Fetzer, F.,Weber, R.Graf, T. Weld Seam Geometry and Electrical Resistance of Laser-Welded, Aluminum-Copper Dissimilar Joints Produced with Spatial Beam Oscillation. Metals. 2018 7. p. 510
[10] Weigl, M.Schmidt, M. Influence of the feed rate and the lateral beam displacement on the joining quality of laser-welded copper-stainless steel connections. Physics Procedia. 2010. p. 53–59
[11] Seibold, M.,Schricker, K.Bergmann, J. P. Characterization of optical spectrum in laser beam welding of dissimilar aluminum-copper joints and time-dependent correlation to process stages. 2019. p. 50
[12] Schmalen, P.Plapper, P. Spectroscopic studies of dissimilar Al-Cu Laser Welding. Manufacturing Sicence and Engineering Conference. 2018
[13] Gao, M.,Chen, C.,Hu, M.,Guo, L.,Wang, Z.Zeng, X. Characteristics of plasma plume in fiber laser welding of aluminum alloy. Applied Surface Science. 2015. p. 181–186
[14] Semrock, I. 485/20 nm BrightLine single-bandpass filter. www.Semrock.com/FilterDetails.aspx?id=FF02-485/20-25
[15] Eriksson E. A. I.,Norman, P.Kaplan, A. F. H. Basic study of photodiode signals from laser welding emissions. 2009
[16] Bagger, C.Olsen, F. O. Laser welding closed-loop power control. Journal of Laser Applications. 2003 1. p. 19–24
[17] Hofmann, K.,Holzer, M.,Hugger, F.,Roth, S.Schmidt, M. Reliable Copper and Aluminum Connections for High Power Applications in Electromobility. Physics Procedia. 2014. p. 601–609
[18] IPG Photonics. SPECIFICATION YTTERBIUM FIBER LASER Model YLR-450/4500-QCW-MM-AC-Y14
[19] Datenblatt - Al99,5 - EN AW-1050A. https://www.alcumet.de/daten/Datenblatt_Al99,5_EN_AW-1050A.pdf
[20] Klöckner & Co, D. DC01 (1.0330). https://facts.kloeckner.de/werkstoffe/stahl/1-0330/, abgerufen am: 14.03.2020
[21] Semiconductor Group, 1998. Silicon Photodiode for the visible spectral range
[22] Chopde, R. S.,Gadewar, S. P.,Khond, M. P.Rathod, M. J. Study on Laser beam Welding of Copper and Aluminum joint. IOSR Journal of Mechanical and Civil Engineering. 2017 10. p. 65–74
[23] Khaskin, V.Y.,Korzhik, V. N.,Chizhskaya, T. G.,Sidorets, V. N.Lo Zie. Effect of laser radiation absorption on efficiency of laser welding of copper and its alloys. The Paton Welding Journal. 2016 11. p. 31–35
[24] Schneider, M.,Berthe, L.,Fabbro, R.Muller, M. Measurement of laser absorptivity for operating parameters characteristic of laser drilling regime. Journal of Physics D: Applied Physics. 2008 15. p.155502